η^6-Coordination of the Curved Carbon Surface of Corannulene ($C_{20}H_{10}$) to (η^6-arene)M^{2+} (M = Ru, Os)

Bolin Zhu,† Arkady Ellern,† Andrzej Sygula,‡ Renata Sygula,‡ and Robert J. Angelici*,†

Ames Laboratory and Department of Chemistry, Iowa State University, Ames, Iowa 50011-3111, and Department of Chemistry, Mississippi State University, Mississippi State, Mississippi 39762

Received November 28, 2006

Reactions of [(η^6-arene)M(acetone)$_3$]X_2 (M = Ru, Os; X = BF_4, PF_6, or SbF_6) with 1 equiv of the curved-surface buckybowl, corannulene ($C_{20}H_{10}$, **1**), in CD_3NO_2 afford quantitatively the η^6-coordinated complexes [(η^6-C_6Me_6)Ru(η^6-$C_{20}H_{10}$)]X_2 (**3a**, X = SbF_6; **3b**, X = PF_6; **3c**, X = BF_4), [(η^6-C_6HMe_5)-Ru(η^6-$C_{20}H_{10}$)]$(SbF_6)_2$ (**4**), [(η^6-C_6EtMe_5)Ru(η^6-$C_{20}H_{10}$)]$(SbF_6)_2$ (**5**), and [(η^6-cymene)Os(η^6-$C_{20}H_{10}$)]$(SbF_6)_2$ (**6**). In the solid state, yellow complexes **3**−**6** are stable in dry air for several months and have all been characterized by their ^1H, $^{13}C\{^1H\}$, and COSY NMR, mass spectra, elemental analyses, and X-ray diffraction; the corannulene in the complexes is slightly flattened as compared with free corannulene, **1**. Even in the presence of excess [(η^6-arene)M(acetone)$_3$]X_2, it was not possible to add two (η^6-arene)M^{2+} units to **1**. The corannulene ligand in **3a** is susceptible to nucleophilic attack by phosphines to give a mixture of adducts.

Introduction

Buckminsterfullerene (C_{60}) and its numerous transition metal complexes[1] have been studied extensively in recent decades; the metal is always bonded to two carbon atoms (η^2). Although C_{60} contains 20 six-membered rings, there are no reported examples of a complex in which C_{60} is η^6-coordinated to a transition metal. In recent years, much interest has been directed toward the synthesis of metal complexes of curved-surface fragments of C_{60}, called buckybowls.[2] The smallest buckybowl is corannulene ($C_{20}H_{10}$, **1**),[3−6] which may be described as the cap of C_{60}.

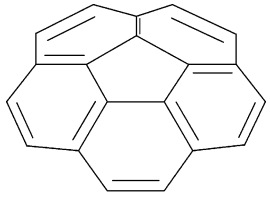

1

Reactions of transition metal complexes with corannulene and its derivatives result in the formation of three major types of corannulene complexes: those with η^6- or η^2-coordinated metals and those in which the metal is σ-bonded to a rim carbon atom. Complexes in which the metal is η^6-coordinated to a six-membered ring are [Cp*Ru(η^6-$C_{20}H_{10}$)][X] (X = $O_3SCF_3^-$, BF_4^-, PF_6^-, or SbF_6^-),[7,8] [(Cp*Ru)$_2$(μ_2-η^6:η^6-$C_{20}H_{10}$)][X]$_2$ (X = BF_4^-, PF_6^-, or SbF_6^-),[8,9] [Cp*Ir(η^6-$C_{20}H_{10}$)][BF_4]$_2$,[10] [(COE)$_2$M(η^6-$C_{20}H_{10}$)][X] (COE = cyclooctene, M = Rh, Ir),[11a] and the acecorannulene complex [Cp*Ru(η^6-$C_{22}H_{12}$)][OTf].[11b] X-ray structural investigations show that the corannulene bowl in [Cp*Ru(η^6-$C_{20}H_{10}$)][SbF_6] is slightly flattened, while the bowl in [(Cp*Ru)$_2$(μ_2-η^6:η^6-$C_{20}H_{10}$)][X]$_2$ (X = PF_6^- and SbF_6^-) is

* To whom correspondence should be addressed. Tel: 515-294-2603. Fax: 515-294-0105. E-mail: angelici@iastate.edu.

† Iowa State University.

‡ Mississippi State University.

(1) For examples see: (a) Lee, K.; Choi, Y. J.; Cho, Y.-J.; Lee, C. Y.; Song, H.; Lee, C. H.; Lee, Y. S.; Park, J. T. *J. Am. Chem. Soc.* **2004**, *126*, 9837. (b) Song, L.-C.; Yu, G.-A.; Su, F.-H.; Hu, Q.-M. *Organometallics* **2004**, *23*, 4192. (c) Song, L.-C.; Wang, G.-F.; Liu, P.-C.; Hu, Q.-M. *Organometallics* **2003**, *22*, 4593. (d) Lee, K.; Song, H.; Kim, B.; Park, J. T.; Park, S.; Choi, M.-G. *J. Am. Chem. Soc.* **2002**, *124*, 2872. (e) Song, L.-C.; Liu, J.-T.; Hu, Q.-M.; Weng, L.-H. *Organometallics* **2000**, *19*, 1643. (f) Balch, A. L.; Olmstead, M. M. *Chem. Rev.* **1998**, *98*, 2123. (g) Hsu, H.-F.; Shapley, J. R. *J. Am. Chem. Soc.* **1996**, *118*, 9192. (h) Fagan, P. J.; Calabrese, J. C.; Malone, B. *Science* **1991**, *252*, 1160. (i) Hirsch, A.; Bretbreich, M. *Fullerenes: Chemistry and Reactions*; Wiley-VCH: Weinheim, 2005.

(2) (a) Sygula, A.; Rabideau, P. W. In *Carbon-Rich Compounds: From Molecules to Materials*; Haley, M. M., Tykwinski, R. R., Eds.; Wiley-VCH: Weinheim, Germany, 2006; p 529. (b) Petrukhina, M. A.; Scott, L. T. *Dalton Trans.* **2005**, 2969. (c) Wu, Y.-T.; Siegel, J. S. *Chem. Rev.* **2006**, *106*, 4843−4867.

(3) (a) Rabideau, P. W.; Abdourazak, A. H.; Folsom, H. E.; Marcinow, Z.; Sygula, A.; Sygula, R. *J. Am. Chem. Soc.* **1995**, *117*, 6410. (b) Abdourazak, A. H.; Marcinow, Z.; Sygula, A.; Sygula, R.; Rabideau, P. W. *J. Am. Chem. Soc.* **1995**, *117*, 6410. (c) Rabideau, P. W.; Sygula, A. *Acc. Chem. Res.* **1996**, *29*, 235.

(4) (a) Barth, W. E.; Lawton, R. G. *J. Am. Chem. Soc.* **1966**, *88*, 380. (b) Lawton, R. G.; Barth, W. E. *J. Am. Chem. Soc.* **1971**, *93*, 1730.

(5) (a) Hanson, J. C.; Nordman, C. E. *Acta Crystallogr., Sect. B: Struct. Sci.* **1976**, *B32*, 1147. (b) Petrukhina, M. A.; Andreini, K. W.; Mack, J.; Scott, L. T. *J. Org. Chem.* **2005**, *70*, 5713.

(6) (a) Sygula, A.; Xu, G.; Marcinow, Z.; Rabideau, P. W. *Tetrahedron* **2001**, *57*, 3637, and references therein. (b) Scott, L. T.; Cheng, P.-C.; Hashemi, M. M.; Bratcher, M. S.; Meyer, D. T.; Warren, H. B. *J. Am. Chem. Soc.* **1997**, *119*, 10963, and references therein. (c) Seiders, T. J.; Baldridge, K. K.; Elliott, E. L.; Grube, G. H.; Siegel, J. S. *J. Am. Chem. Soc.* **1999**, *121*, 7439. (d) Seiders, T. J.; Elliott, E. L.; Grube, G. H.; Siegel, J. S. *J. Am. Chem. Soc.* **1999**, *121*, 7804. (e) Jones, C. S.; Elliot, E. L.; Siegel, J. S. *Synlett* **2004**, 187.

(7) Seiders, T. J.; Baldridge, K. K.; O'Connor, J. M.; Siegel, J. S. *J. Am. Chem. Soc.* **1997**, *119*, 4781.

(8) Vecchi, P. A.; Alvarez, C. M.; Ellern, A.; Angelici, R. J.; Sygula, A.; Sygula, R.; Rabideau, P. W. *Organometallics* **2005**, *24*, 4543.

(9) Vecchi, P. A.; Alvarez, C. M.; Ellern, A.; Angelici, R. J.; Sygula, A.; Sygula, R.; Rabideau, P. W. *Angew. Chem., Int. Ed.* **2004**, *43*, 4497.

(10) Alvarez, C. M.; Angelici, R. J.; Sygula, A.; Sygula, R.; Rabideau, P. W. *Organometallics* **2003**, *22*, 624.

(11) (a) Siegel, J. S.; Baldridge, K. K.; Linden, A.; Dorta, R. *J. Am. Chem. Soc.* **2006**, *128*, 10644−10645. (b) Seiders, T. J.; Baldridge, K. K.; O'Connor, J. M.; Siegel, J. S. *Chem. Commun.* **2004**, 950.

10.1021/om0610795 CCC: $37.00
Publication on Web 03/01/2007

greatly flattened or essentially flat, depending on the anion. Complexes of η^2-coordinated corannulene, $[[Rh_2(O_2CCF_3)_4]_m \cdot (C_{20}H_{10})_n]$ (m:n = 1:1 and 3:2) and $Ru_2(O_2CCF_3)_2(CO)_4 \cdot (\eta^2\text{-}C_{20}H_{10})_2$, were prepared by a gas-phase deposition method.[12] X-ray structural investigations of these compounds show that the M_2 units are η^2-coordinated to the *exo* or both the *exo* and *endo* sides of the corannulene in one- and two-dimensional arrays. The structures of the corannulene units in the compounds were not significantly different than that of free corannulene.[5] Also, corannulene complexes of AgX ($X^- = ClO_4^-$, $CF_3SO_3^-$, or BF_4^-), characterized by X-ray diffraction, were shown to exist as one- or two-dimensional networks in which Ag^+ and corannulene are linked by η^2 and η^1 coordination; the structure of the corannulene unit in these compounds is changed very little from that of free corannulene.[13] The third type of corannulene complex is that in which a C−H hydrogen in $C_{20}H_{10}$ is replaced by a metal, as in $(\eta^1\text{-}C_{20}H_9)M(PEt_3)_2Br$ (M = Ni, Pt).[14] In the present study, we sought to prepare η^6-corannulene complexes of the type $M(\eta^6\text{-arene})(\eta^6\text{-}C_{20}H_{10})^{2+}$ (M = Ru, Os) in order to evaluate their stabilities, to determine the effect of the $M(\eta^6\text{-arene})^{2+}$ unit on the shape of the corannulene, and to explore the possibility that the $M(\eta^6\text{-arene})^{2+}$ unit promotes the attack of nucleophiles on the coordinated corannulene.

Experimental Section

General Considerations. All reactions were carried out under an atmosphere of dry argon using standard Schlenk techniques. Methylene chloride (CH_2Cl_2), diethyl ether (Et_2O), and hexanes were purified on alumina using a Solv-Tek solvent purification system. Acetone was refluxed overnight with anhydrous calcium sulfate, distilled, and subjected to three freeze−pump−thaw cycles before use. Methylene chloride-d_2 (CD_2Cl_2) was refluxed overnight with calcium hydride, distilled, and subjected to three freeze−pump−thaw cycles before use. Nitromethane-d_3 (CD_3NO_2) was purchased from Aldrich and subjected to three freeze−pump−thaw cycles before use. Corannulene (**1**),[6a] $[(\eta^6\text{-}C_6Me_6)RuCl_2]_2$,[15] $[(\eta^6\text{-}C_6HMe_5)RuCl_2]_2$,[16] $[(\eta^6\text{-cymene})OsCl_2]_2$,[17] and C_6EtMe_5[18] were synthesized following published methods. All other chemicals ($AgBF_4$, $AgPF_6$, $AgSbF_6$, 99.99+%) were used as purchased from Aldrich without further purification. Filtrations were performed through a small plug of filter paper, Celite, and cotton, and the solutions were transferred via thin-wall Teflon tubing (Alpha Wire Corporation).

Solution NMR spectra were obtained at room temperature on a Bruker DRX-400 spectrometer using the solvent as the internal lock and internal reference [δ = 4.33 (^{1}H), 62.8 ppm (^{13}C) for CD_3NO_2 and 5.32 (^{1}H), 54.0 ppm (^{13}C) for CD_2Cl_2]. Electrospray ionization mass spectra were obtained on a Finnigan TSQ700 triple quadrupole mass spectrometer (Finnigan MAT, San Jose, CA) fitted with a Finnigan ESI interface. Elemental analyses were performed on a Perkin-Elmer 2400 series II CHNS/O analyzer.

Synthesis of $[(\eta^6\text{-}C_6EtMe_5)RuCl_2]_2$ (2). A mixture of $[(\eta^6\text{-cymene})RuCl_2]_2$ (300 mg, 0.49 mmol) and ethylpentamethylbenzene (3.0 g, 17.0 mmol) was stirred at 180−185 °C for 3.5 h under an argon atmosphere. After the melt was allowed to cool to room temperature to give a solid, *p*-cymene and some of the excess ethylpentamethylbenzene were removed by washing with hexanes, and the remaining dark orange solid was then recrystallized from chloroform/hexanes to give dark red crystals of $[(\eta^6\text{-}C_6EtMe_5)RuCl_2]_2$ (307 mg, 90%). ^{1}H NMR (400.13 MHz, $CDCl_3$): δ 2.59 (q, J = 7.6 Hz, 2H), 2.04 (s, 6H), 2.003 (s, 6H), 1.995 (s, 3H), 1.02 (t, J = 7.6 Hz, 3H) ppm. $^{13}C\{^1H\}$ NMR (100.61 MHz, $CDCl_3$): δ 93.00, 90.32, 89.80, 89.58, 23.30, 16.22, 16.03, 15.14, 12.22 ppm. MS: m/z 661 (M − Cl). Anal. Calcd for $C_{26}H_{40}Cl_4Ru_2$: C, 44.83; H, 5.79. Found: C, 44.69; H, 6.01.

General Procedure for the Preparation of the $[(\eta^6\text{-Arene})M(\eta^6\text{-}C_{20}H_{10})][X]_2$ Complexes (3−6). To a solution of 0.020 mmol of $[(\eta^6\text{-arene})MCl_2]_2$ (arene = C_6Me_6, C_6HMe_5, C_6EtMe_5, M = Ru, or arene = cymene, M = Os) in 3 mL of acetone was added 0.081 mmol of AgX (X = SbF_6, PF_6, or BF_4). After the solution was stirred at room temperature for 10 min, the AgCl precipitate was filtered off, and the yellow solution was added to 0.040 mmol of corannulene. This solution was evaporated to dryness under vacuum, and the residue was dissolved in 1 mL of CD_3NO_2. The solution was stirred at 60 °C for 0.5 h and then concentrated under vacuum; the product was precipitated by addition of 10 mL of Et_2O. The residue was washed with Et_2O (2 × 3 mL) and dried under vacuum to give $[(\eta^6\text{-arene})M(\eta^6\text{-}C_{20}H_{10})][X]_2$ quantitatively as a yellow powder.

Characterization of Compounds 3−6. $[(\eta^6\text{-}C_6Me_6)Ru(\eta^6\text{-}C_{20}H_{10})][SbF_6]_2$ (3a). ^{1}H NMR (400.13 MHz, CD_3NO_2): δ 8.73 (d, J_{H2-H3} = 8.8 Hz, H3-$C_{20}H_{10}$, 2H), 8.43 (d, J_{H4-H5} = 8.8 Hz, H5-$C_{20}H_{10}$, 2H), 8.21 (d, J_{H5-H4} = 8.8 Hz, H4-$C_{20}H_{10}$, 2H), 7.80 (d, J_{H3-H2} = 8.8 Hz, H2-$C_{20}H_{10}$, 2H), 7.48 (s, H1-$C_{20}H_{10}$, 2H), 2.35 (s, C_6Me_6, 18H) ppm. $^{13}C\{^1H\}$ NMR (100.61 MHz, CD_3NO_2): δ 144.1 (C11), 143.7 (C3), 138.1 (C9), 136.3 (C10), 136.0 (C8), 134.9 (C5), 131.6 (C4), 122.4 (C2), 109.8 (C6), 106.4 (C_6Me_6), 98.1 (C7), 92.3 (C1), 17.6 (Me) ppm. MS: m/z 513 ($[(\eta^6\text{-}C_6Me_6)Ru(\eta^6\text{-}C_{20}H_{10})]^+$, 100%), 257 ($[(\eta^6\text{-}C_6Me_6)Ru(\eta^6\text{-}C_{20}H_{10})]^{2+}$, 5%) electrospray in CH_3NO_2. Anal. Calcd for $C_{32}H_{28}F_{12}RuSb_2$: C, 39.01; H, 2.86. Found: C, 38.90; H, 3.14.

$[(\eta^6\text{-}C_6Me_6)Ru(\eta^6\text{-}C_{20}H_{10})][PF_6]_2$ (3b). ^{1}H NMR (400.13 MHz, CD_3NO_2): δ 8.72 (d, J_{HH} = 8.8 Hz, $C_{20}H_{10}$, 2H), 8.43 (d, J_{HH} = 8.8 Hz, $C_{20}H_{10}$, 2H), 8.20 (d, J_{HH} = 8.8 Hz, $C_{20}H_{10}$, 2H), 7.78 (d, J_{HH} = 8.8 Hz, $C_{20}H_{10}$, 2H), 7.47 (s, $C_{20}H_{10}$, 2H), 2.34 (s, C_6Me_6, 18H) ppm. MS: m/z 513 ($[(\eta^6\text{-}C_6Me_6)Ru(\eta^6\text{-}C_{20}H_{10})]^+$, 100%), 257 ($[(\eta^6\text{-}C_6Me_6)Ru(\eta^6\text{-}C_{20}H_{10})]^{2+}$, 5%) electrospray in CH_3NO_2. Anal. Calcd for $C_{32}H_{28}F_{12}P_2Ru$: C, 47.83; H, 3.51. Found: C, 47.54; H, 3.79.

$[(\eta^6\text{-}C_6Me_6)Ru(\eta^6\text{-}C_{20}H_{10})][BF_4]_2$ (3c). ^{1}H NMR (400.13 MHz, CD_3NO_2): δ 8.72 (d, J_{HH} = 8.8 Hz, $C_{20}H_{10}$, 2H), 8.43 (d, J_{HH} = 8.8 Hz, $C_{20}H_{10}$, 2H), 8.20 (d, J_{HH} = 8.8 Hz, $C_{20}H_{10}$, 2H), 7.80 (d, J_{HH} = 8.8 Hz, $C_{20}H_{10}$, 2H), 7.50 (s, $C_{20}H_{10}$, 2H), 2.35 (s, C_6Me_6, 18H) ppm. MS: m/z 513 ($[(\eta^6\text{-}C_6Me_6)Ru(\eta^6\text{-}C_{20}H_{10})]^+$, 100%), 257 ($[(\eta^6\text{-}C_6Me_6)Ru(\eta^6\text{-}C_{20}H_{10})]^{2+}$, 3%) electrospray in CH_3NO_2. Anal. Calcd for $C_{32}H_{28}B_2F_8Ru \cdot CH_3NO_2$: C, 52.97; H, 4.18. Found: C, 52.86; H, 4.51.

$[(\eta^6\text{-}C_6HMe_5)Ru(\eta^6\text{-}C_{20}H_{10})][SbF_6]_2$ (4). ^{1}H NMR (400.13 MHz, CD_3NO_2): δ 8.70 (d, J_{HH} = 8.8 Hz, $C_{20}H_{10}$, 2H), 8.41 (d, J_{HH} = 8.8 Hz, $C_{20}H_{10}$, 2H), 8.18 (d, J_{HH} = 8.8 Hz, $C_{20}H_{10}$, 2H), 7.77 (d, J_{HH} = 8.8 Hz, $C_{20}H_{10}$, 2H), 7.53 (s, $C_{20}H_{10}$, 2H), 6.76 (s, 1H), 2.37 (s, 6H), 2.19 (s, 6H), 2.16 (s, 3H) ppm. MS: m/z 499 ($[(\eta^6\text{-}C_6HMe_5)Ru(\eta^6\text{-}C_{20}H_{10})]^+$, 5%), 249 ($[(\eta^6\text{-}C_6HMe_5)Ru(\eta^6\text{-}C_{20}H_{10})]^{2+}$, 100%) electrospray in CH_3NO_2. Anal. Calcd for $C_{31}H_{26}F_{12}RuSb_2$: C, 38.34; H, 2.70. Found: C, 38.33; H, 2.72.

$[(\eta^6\text{-}C_6EtMe_5)Ru(\eta^6\text{-}C_{20}H_{10})][SbF_6]_2$ (5). ^{1}H NMR (400.13 MHz, CD_3NO_2): δ 8.72 (d, J_{HH} = 8.8 Hz, $C_{20}H_{10}$, 2H), 8.43 (d, J_{HH} = 8.8 Hz, $C_{20}H_{10}$, 2H), 8.20 (d, J_{HH} = 8.8 Hz, $C_{20}H_{10}$, 2H), 7.78 (d, J_{HH} = 8.8 Hz, $C_{20}H_{10}$, 2H), 7.48 (s, $C_{20}H_{10}$, 2H), 2.70 (q, J = 7.6 Hz, 2H), 2.35 (s, 9H), 2.33 (s, 6H), 1.18 (t, J = 7.6 Hz,

(12) (a) Petrukhina, M. A.; Andreini, K. W.; Mack, J.; Scout, L. T. *Angew. Chem., Int. Ed.* **2003**, *42*, 3375. (b) Petrukhina, M. A.; Sevryugina, Y.; Rogachev, A. Y.; Jackson, E. A.; Scott, L. T. *Organometallics* **2006**, *25*, 5492.

(13) Elliott, E. L.; Hernández, G. A.; Linden, A.; Siegel, J. S. *Org. Biomol. Chem.* **2005**, *3*, 407.

(14) Lee, H. B.; Sharp, P. R. *Organometallics* **2005**, *24*, 4875.

(15) Bennett, M. A.; Huang, T.-N.; Matheson, T. W.; Smith, A. K. *Inorg. Synth.* **1982**, *21*, 74.

(16) Older, C. M.; Stryker, J. M. *Organometallics* **1998**, *17*, 5596.

(17) Werner, H.; Zenkert, K. *J. Organomet. Chem.* **1988**, *345*, 151.

(18) Kiprof, P.; Li, J.; Renish, C. L.; Kalombo, E. K.; Young, V. G., Jr. *J. Organomet. Chem.* **2001**, *620*, 113.

Table 1. Crystal Data and Structure Refinement for 3a, 4, 5, and 6·CH_2Cl_2

	$[(\eta^6\text{-}C_6Me_6)Ru(\eta^6\text{-}C_{20}H_{10})][SbF_6]_2$ (**3a**)	$[(\eta^6\text{-}C_6HMe_5)Ru(\eta^6\text{-}C_{20}H_{10})][SbF_6]_2$ (**4**)
empirical formula	$C_{32}H_{28}F_{12}RuSb_2$	$C_{31}H_{26}F_{12}RuSb_2$
fw	985.11	971.09
cryst syst	orthorhombic	orthorhombic
space group	*Pbca*	*Pbca*
unit cell dimens	$a = 17.793(4)$ Å	$a = 18.030(4)$ Å
	$b = 15.863(4)$ Å	$b = 15.110(3)$ Å
	$c = 23.310(5)$ Å	$c = 23.476(5)$ Å
	$\alpha = 90°$	$\alpha = 90°$
	$\beta = 90°$	$\beta = 90°$
	$\gamma = 90°$	$\gamma = 90°$
volume	6580(3) Å^3	6396(2) Å^3
Z	8	8
density (calcd)	1.989 Mg/m^3	2.017 Mg/m^3
abs coeff	2.174 mm^{-1}	2.235 mm^{-1}
F(000)	3792	3728
no. of reflns collected	52 421	30 578
max. and min. transmn	1 and 0.78	1 and 0.74
no. of data/restraints/ params	6727/0/430	3348/0/420
goodness-of-fit on F^2	1.150	1.101
final R^a indices [$I > 2\sigma(I)$]	R1 = 0.0596, wR2 = 0.1521	R1 = 0.0339, wR2 = 0.0815
R^a indices (all data)	R1 = 0.0905, wR2 = 0.1753	R1 = 0.0419, wR2 = 0.0881
largest diff peak and hole	3.418 and −1.590 e Å^{-3}	1.558 and −0.970 e Å^{-3}

	$[(\eta^6\text{-}C_6EtMe_5)Ru(\eta^6\text{-}C_{20}H_{10})][SbF_6]_2$ (**5**)	$[(\eta^6\text{-cymene})Os(\eta^6\text{-}C_{20}H_{10})][SbF_6]_2\cdot CH_2Cl_2$ (**6**·CH_2Cl_2)
empirical formula	$C_{33}H_{30}F_{12}RuSb_2$	$C_{31}H_{26}Cl_2F_{12}OsSb_2$
fw	999.14	1131.12
cryst syst	orthorhombic	monoclinic
space group	*Pbca*	*C*2/*c*
unit cell dimens	$a = 17.783(4)$ Å	$a = 36.205(8)$ Å
	$b = 16.056(3)$ Å	$b = 9.510(2)$ Å
	$c = 23.270(5)$ Å	$c = 25.232(6)$ Å
	$\alpha = 90°$	$\alpha = 90°$
	$\beta = 90°$	$\beta = 128.968(8)°$
	$\gamma = 90°$	$\gamma = 90°$
volume	6644(2) Å^3	6755(3) Å^3
Z	8	8
density (calcd)	1.998 Mg/m^3	2.225 Mg/m^3
abs coeff	2.155 mm^{-1}	5.589 mm^{-1}
F(000)	3856	4256
no. of reflns collected	54 714	30 178
max. and min. transmn	1 and 0.79	1 and 0.51
no. of data/restraints/ params	8001/0/439	7996/2/437
goodness-of-fit on F^2	1.029	1.041
final R^a indices [$I > 2\sigma(I)$]	R1 = 0.0400, wR2 = 0.0976	R1 = 0.0637, wR2 = 0.1846
R^a indices (all data)	R1 = 0.0613, wR2 = 0.1157	R1 = 0.0974, wR2 = 0.2148
largest diff peak and hole	3.011 and −1.474 e Å^{-3}	3.875 and −2.259 e Å^{-3}

[a] $R1 = \sum||F_o| - |F_c||/\sum|F_o|$ and $wR2 = \{\sum[w(F_o^2 - F_c^2)^2]/\sum[w(F_o^2)^2]\}^{1/2}$.

3H) ppm. MS: *m*/*z* 527 ($[(\eta^6\text{-}C_6EtMe_5)Ru(\eta^6\text{-}C_{20}H_{10})]^+$, 4%), 264 ($[(\eta^6\text{-}C_6EtMe_5)Ru(\eta^6\text{-}C_{20}H_{10})]^{2+}$, 100%) electrospray in CH_3NO_2. Anal. Calcd for $C_{33}H_{30}F_{12}RuSb_2$: C, 39.67; H, 3.03. Found: C, 39.36; H, 3.08.

$[(\eta^6\text{-cymene})Os(\eta^6\text{-}C_{20}H_{10})][SbF_6]_2$ (6). ^{1}H NMR (400.13 MHz, CD_2Cl_2): δ 8.72 (d, J_{HH} = 8.8 Hz, H3-$C_{20}H_{10}$, 2H), 8.39 (d, J_{HH} = 8.8 Hz, H5-$C_{20}H_{10}$, 2H), 8.10 (d, J_{HH} = 8.8 Hz, H4-$C_{20}H_{10}$, 2H), 7.91 (s, H1-$C_{20}H_{10}$, 2H), 7.80 (d, J_{HH} = 8.8 Hz, H2-$C_{20}H_{10}$, 2H), 7.05 (d, 2H, J = 6.4 Hz, 2H), 7.00 (d, 2H, J = 6.4 Hz, 2H), 2.53 (sep, J = 6.8 Hz, 1H), 2.47 (s, 3H), 1.13 (d, J = 7.2 Hz, 6H) ppm. MS: *m*/*z* 287 ($[(\eta^6\text{-cymene})Os(\eta^6\text{-}C_{20}H_{10})]^{2+}$, 100%) electrospray in CH_3NO_2. Anal. Calcd for $C_{30}H_{24}F_{12}OsSb_2$: C, 34.44; H, 2.31. Found: C, 34.17; H, 2.37.

X-ray Structural Determinations of $[(\eta^6\text{-}C_6Me_6)Ru(\eta^6\text{-}C_{20}H_{10})][SbF_6]_2$ (3a), $[(\eta^6\text{-}C_6HMe_5)Ru(\eta^6\text{-}C_{20}H_{10})][SbF_6]_2$ (4), $[(\eta^6\text{-}C_6EtMe_5)Ru(\eta^6\text{-}C_{20}H_{10})][SbF_6]_2$ (5), and $[(\eta^6\text{-cymene})Os(\eta^6\text{-}C_{20}H_{10})][SbF_6]_2\cdot CH_2Cl_2$ (6·CH_2Cl_2). Orange crystals of complexes **3a**, **4**, and **5** suitable for X-ray diffraction study were grown by recrystallization from a saturated CH_3NO_2 solution of the complex that was surrounded by Et_2O and stored at room temperature for 3 days. Yellow crystals of complex **6**·CH_2Cl_2 were grown by recrystallization from a saturated CH_2Cl_2 solution of the complex that was surrounded by pentane and stored at room temperature for 3 days.

The crystals were selected under ambient conditions, coated in epoxy, and mounted on the end of a glass fiber. Crystal data collections were performed at 193 K on a Bruker CCD-1000 diffractometer with Mo Kα (λ = 0.71073 Å) radiation and a detector-to-crystal distance of 5.03 cm. Data were collected using the full sphere routine (ω-scan, 1860 frames with 0.3 deg width) and were corrected for Lorentz and polarization effects. The absorption corrections were based on fitting a function to the empirical transmission surface as sampled by multiple equivalent measurements using SADABS software.[19] Positions of the heavy atoms were found by direct methods. The remaining atoms were located in an alternating series of least-squares cycles and difference Fourier maps. All non-hydrogen atoms were refined using a full-matrix anisotropic approximation. All hydrogen atoms were placed

(19) Blessing, R. H. *Acta Crystallogr.* **1995**, *A51*, 33.

Table 2. Assigned Experimental Chemical Shifts for 3a and Calculated Values

	C1	C2	C3	C4	C5	C6	C7	C8	C9	C10	C11
δ (ppm), exptl	92.3	122.4	143.7	131.6	134.9	109.8	98.1	136.0	138.1	136.3	144.1
δ (ppm), calcd	86.3	114.9	143.3	128.2	134.5	106.7	91.8	128.7	131.9	130.1	136.0

in the structure factor calculation at idealized positions and refined using a riding model. Other crystallographic data are given in Table 1.

Computational Details. Computational studies were undertaken for the model dications [(η^6-C_6Me_6)Ru(η^6-$C_{20}H_{10}$)]$^{2+}$ ($\mathbf{3}^{2+}$), [(η^6-C_6HMe_5)Ru(η^6-$C_{20}H_{10}$)]$^{2+}$ ($\mathbf{4}^{2+}$), [(η^6-C_6EtMe_5)Ru(η^6-$C_{20}H_{10}$)]$^{2+}$ ($\mathbf{5}^{2+}$), and [(η^6-cymene)Os(η^6-$C_{20}H_{10}$)]$^{2+}$ ($\mathbf{6}^{2+}$). The calculations were performed by employing the Gaussian03 program package.[20] Hybrid density functional theory was used at the B3LYP (i.e., Becke's three-parameter hybrid exchange functional[21] in combination with Lee−Yang−Paar nonlocal correlation functional[22]) and Perdew−Burke−Erzenhof exchange−correlation functional (PBE) levels.[23] Full geometry optimizations were performed by employing a standard 6-31G(d) basis set for carbon and hydrogen atoms, while the pseudopotential basis sets of Hay and Wadt were used for the metal centers.[24] These levels of theory are hereafter referred to as B3LYP/GEN and PBE/GEN. X-ray geometries of the appropriate fragments were used as starting points for geometry optimization procedures. The gauge-independent atomic orbital (GIAO) method[25] was used for NMR chemical shift calculations, as implemented in Gaussian03.

Results and Discussion

Synthesis of [(η^6-C_6Me_6)Ru(η^6-$C_{20}H_{10}$)]X_2 (3a, X = SbF_6; 3b, X = PF_6; 3c, X = BF_4), [(η^6-C_6HMe_5)Ru(η^6-$C_{20}H_{10}$)]-(SbF_6)$_2$ (4), [(η^6-C_6EtMe_5)Ru(η^6-$C_{20}H_{10}$)](SbF_6)$_2$ (5), and [(η^6-cymene)Os(η^6-$C_{20}H_{10}$)](SbF_6)$_2$ (6). Mixed arene complexes [Ru(η^6-arene)(η^6-arene′)]$^{2+}$ were first prepared by Bennett et al.[26] by reacting [(η^6-arene)$RuCl_2$]$_2$ with acetone and $AgBF_4$ and then adding arene′ in CF_3COOH[15,26−28] or in CH_2Cl_2[29] solvent. This procedure was extended later to the synthesis of the osmium analogues.[30,31] Complexes **3**−**6** were synthesized by the same general method (eq 1).

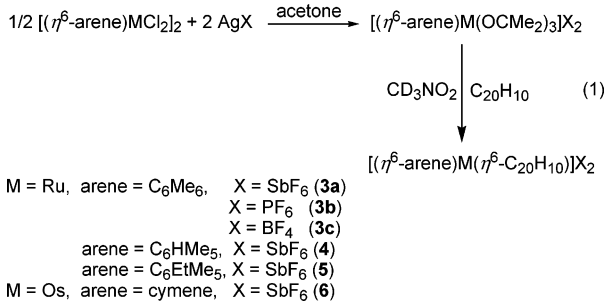

In the second step, CD_3NO_2 was chosen as the solvent because of its weak coordinating ability, its ability to solubilize the products, and our previous success in preparing [Cp*Ru(η^6-$C_{20}H_{10}$)]X complexes in this solvent.[8] Attempts to prepare [{(η^6-C_6Me_6)Ru}$_2$(μ_2-η^6:η^6-$C_{20}H_{10}$)]$^{4+}$ by using 2 equiv of (η^6-C_6Me_6)Ru$(OCMe_2)_3^{2+}$ were unsuccessful; they yielded only **3a**. Attempts to prepare (η^6-arene)Ru(η^6-$C_{20}H_{10}$)$^+$, where η^6-arene is C_6H_6, 1,3,5-$Me_3C_6H_3$, or cymene, gave impure, oily products that decomposed upon purification. Complexes **3**−**6** are yellow solids that are stable in dry air for several months without apparent decomposition. In our experience, these are the most stable η^6-corannulene complexes reported to date and are considerably more stable than the previously reported [Cp*Ru(η^6-$C_{20}H_{10}$)][X] (X = BF_4, PF_6, or SbF_6),[7,8] [Cp*Ir(η^6-$C_{20}H_{10}$)]-$[BF_4]_2$,[10] and [Cp*Ir(η^6-$C_{20}H_6Me_4$)]$[BF_4]_2$,[10] which are very sensitive to moisture. However, the corannulene is displaced when **3b** is reacted with benzene, acetone, or acetonitrile (20 equiv) in CD_3NO_2 at room temperature. The half-life for corannulene displacement by benzene is 4 days, by acetone is 16 h, and by acetonitrile is 5 h. These half-lives are much longer than those for corannulene displacement in [Cp*Ir(η^6-$C_{20}H_{10}$)]-$[BF_4]_2$,[10] which is completely substituted by benzene (10 equiv) within 6 h and by acetone (10 equiv) within 4 h.

^{1}H and ^{13}C NMR Spectra of the [(η^6-arene)M(η^6-$C_{20}H_{10}$)-[X]$_2$ Complexes. A full assignment of ^{1}H and ^{13}C NMR resonances for **3a** was achieved using COSY, NOESY, and HMQC data as well as GIAO calculations. Thus, using the singlet ^{1}H NMR absorption at 7.48 ppm as a starting point, the remaining proton signals were assigned by COSY and NOESY experiments. Tertiary carbon atoms were assigned next by an HMQC experiment. Comparison of these assigned ^{13}C carbon atoms with the GIAO-calculated chemical shifts for the model dication [(η^6-C_6Me_6)Ru(η^6-$C_{20}H_{10}$)]$^{2+}$ reveals that the latter are systematically lower than the experimental values but that the trends are nicely reproduced (Table 2). Therefore, using the computed shifts we tentatively assigned quaternary carbons as shown in Figure 1 and Table 2. The assignment was confirmed by an HMBC experiment, which showed the expected pattern of cross-peaks arising mostly from ^3J(C,H) coupling (the experiment was optimized for the couplings of ca. 6 Hz, which is a typical three-bond C, H coupling in aromatic systems; some relatively weak ^2J(C,H) and not completely suppressed ^1J(C,H) cross-peaks can also be seen). Quaternary carbon atoms have not been assigned for previously reported corannulene complexes.[7−11]

A comment about the calculated versus experimental ^{13}C NMR chemical shifts (Table 2) is appropriate here. Even though the match is not quantitatively perfect, it is still very useful for an assignment of spectra. One has to keep in mind that the calculations were performed for the isolated dication, which is a very rough approximation of the real system. Obviously, the

(20) Frisch, M. J.; et al. *Gaussian 03*, Revision D.01; Gaussian, Inc.: Wallingford, CT, 2004.
(21) Becke, A. D. *J. Chem. Phys.* **1993**, *98*, 5648.
(22) Lee, C.; Yang, W.; Parr, R. G. *Phys. Rev.* **1988**, *B37*, 785.
(23) (a) Perdew, J. P.; Burke, K.; Erzenhof, M. *Phys. Rev. Lett.* **1996**, *77*, 3865. (b) Perdew, J. P.; Burke, K.; Erzenhof, M. *Phys. Rev. Lett.* **1997**, *78*, 1396.
(24) Hay, P. J.; Wadt, W. R. *J. Phys. Chem.* **1985**, *82*, 299.
(25) Ditchfield, R. *Mol. Phys.* ***1974***, *27*, 789. Wolinski, K.; Hinton, J. F.; Pulay, P. *J. Am. Chem. Soc.* **1990**, *112*, 8251.
(26) (a) Bennett, M. A.; Smith, A. K. *J. Chem. Soc., Dalton Trans.* **1974**, 233. (b) Bennett, M. A.; Matheson, T. W. *J. Organomet. Chem.* **1979**, *175*, 87.
(27) (a) Suravajjala, S.; Polam, J. R.; Porter, L. C. *Organometallics* **1994**, *13*, 37. (b) Porter, L. C.; Bodige, S.; Selnau, H. E., Jr. *Organometallics* **1995**, *14*, 4222.
(28) Satou, T.; Takehara, K.; Hirakida, M; Sakamoto, Y.; Takemura, H.; Miura, H.; Tomonou, M.; Shinmyozu, T. *J. Organomet. Chem.* **1999**, *577*, 58, and references therein.
(29) (a) Porter, L. C.; Polam, J. R.; Mahmoud, J. *Organometallics* **1994**, *13*, 2092. (b) Porter, L. C.; Polam, J. R.; Bodige, S. *Inorg. Chem.* **1995**, *34*, 998.
(30) (a) Elsegood, M. R. J.; Tocher, D. A. *J. Organomet. Chem.* **1990**, *391*, 239. (b) Elsegood, M. R. J.; Tocher, D. A. *Polyhedron* **1995**, *14*, 3147.
(31) (a) Freedman, D. A.; Matachek, J. R.; Mann, K. R. *Inorg. Chem.* **1993**, *32*, 1078. (b) Freedman, D. A.; Magneson, D. J.; Mann, K. R. *Inorg. Chem.* **1995**, *34*, 2617.
(32) Ward, M. D.; Johnson, D. C. *Inorg. Chem.* **1987**, *26*, 4213.

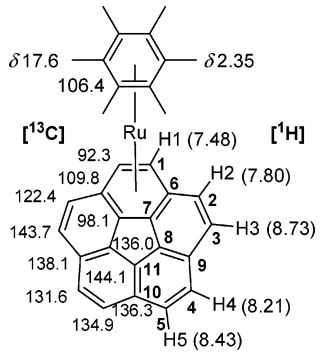

Figure 1. ^{1}H and ^{13}C{1H} NMR spectral assignments for **3a** deduced from COSY, NOESY, HMQC, and HMBC data. Chemical shift values (δ) are in ppm relative to TMS.

presence of counterions and solvents will affect the electron distribution in **3a** and consequently the chemical shifts of its carbon atoms. However, the applied theoretical model seems to reproduce the relative shift changes upon complexation very nicely and can be a useful tool for analysis of experimental spectra.

Proton resonances for hydrogens on corannulene in [(η^6-C_6Me_6)Ru(η^6-$C_{20}H_{10}$)][SbF_6]$_2$ (**3a**), [(η^6-cymene)Os(η^6-$C_{20}H_{10}$)][SbF_6]$_2$ (**6**), [Cp*Ir(η^6-$C_{20}H_{10}$)][BF_4]$_2$,[10] and [Cp*Ru(η^6-$C_{20}H_{10}$)][O_3SCF_3][7] are listed in Table 3. The metal fragment causes δ_{H1} values for the protons on the η^6-coordinated ring to decrease in the following order: Cp*Ir^{2+} (7.98 ppm) > (η^6-C_6Me_6)Ru^{2+} (7.48 ppm) > Cp*Ru^+ (6.59 ppm). Thus, the lower the positive charge on the complex, the further upfield are these protons. This effect of charge on δ_H values of protons in noncoordinated rings follows a similar trend, but the differences between +2 and +1 complexes are less pronounced.

Structural Characterization of the [(η^6-arene)M(η^6-$C_{20}H_{10}$)]-[X]$_2$ Complexes. The structures of complexes **3a**, **4**, **5**, and **6** have been determined from single-crystal X-ray analyses and are shown, along with their C−C bond distances, in Figures 2−5, respectively. In each +2 cation, an (η^6-arene)M^{2+} unit is coordinated to the *exo*-side of a curved corannulene. Our computational studies show that structural parameters of the corannulene in $\mathbf{3}^{2+}$, $\mathbf{4}^{2+}$, and $\mathbf{5}^{2+}$ are practically unaffected by the different arene ligands. Differences in calculated bond lengths of related bonds in the complexes are the same within approximately 0.001 Å. Also, even though the complexes do not exhibit any symmetry in the crystal, the calculated structures of the dications exhibit an approximate C_s symmetry of the corannulene unit in all cases studied. Therefore, we decided to use averaged values of the bond lengths and pyramidalization angles taken from the crystal structures of **3a**, **4**, and **5**, hoping to obtain a more representative picture of structural effects caused by (η^6-arene)Ru^{2+} complexation on the corannulene core by eliminating some of the experimental errors and/or crystal-packing effects. These average values are used in the following discussion of bond distances and POAV values.

The average C−C(ring) bond distances in the (η^6-arene)Ru^{2+} fragment of complexes **3a**, **4**, and **5** are 1.430(13), 1.415(12), and 1.428(7) Å, respectively, which are the same within experimental error as that (1.426(6) Å) in [(η^6-C_6Me_6)$_2$Ru]$^{2+}$.[32] These distances are slightly longer than the value (1.39(2) Å) reported for free hexamethylbenzene.[33] The average Ru−C bond distances in the (η^6-arene)Ru^{2+} unit are 2.222(9), 2.213(8), and 2.221(5) Å, respectively, which are similar to that (2.257(4) Å) in [(η^6-C_6Me_6)$_2$Ru]$^{2+}$. In complex **6**, the average C−C(ring) and Os−C bond distances are 1.422(19) and 2.216(13) Å, which are both in the range reported for other (η^6-arene)Os complexes;[30a,34−36] typical Os−C bond distances lie in the range 2.15−2.25 Å, as in [Os(η^6-C_6H_6)(η^6-[2$_2$](1,4)$C_{16}H_{16}$)]$^{2+}$ (2.21-(2) Å)[30a] and (*p*-cymene)Os(Me_2SO)Cl_2 (2.192(9) Å).[35]

Of special interest is the partial flattening of the corannulene. This distortion of the corannulene curvature is most evident in the π-orbital axis vector (POAV) analysis, which is a method of quantifying the curvature of carbon networks in nonplanar ring systems. In free corannulene, the five core carbon atoms are the most pyramidalized, having POAV values of 8.4°, while the five rim quaternary carbon atoms are less pyramidalized and have POAV values of 3.8° (Figure 6). For comparison, average POAV values in **3a**, **4**, and **5**, assuming C_s symmetry of the corannulene subunit, are also given in Figure 6. The core carbons bonded to Ru have POAV angles that are slightly reduced to 6.8°, as compared with the other three core carbons, which have POAV values (8.7°, 9.4°) that are slightly larger than those of free corannulene (Figure 6). The two rim quaternary carbon atoms that are coordinated to (η^6-arene)Ru^{2+} also have smaller POAV values (1.6°) than in free **1** (3.8°), while those that are not attached to the (η^6-arene)Ru^{2+} unit have POAV values (4.1°, 3.7°) that are similar to those in free **1**. In the previously reported structure of [(Cp*Ru)(η^6-$C_{20}H_{10}$)]-[SbF_6],[9] the core carbons bonded to Ru have POAV angles (6.7°) that are essentially identical to the average values (6.8°) for the three [(η^6-arene)Ru(η^6-$C_{20}H_{10}$)]$^{2+}$ complexes (**3a**, **4**, and **5**). The other core carbons in [(Cp*Ru)(η^6-$C_{20}H_{10}$)][SbF_6] have POAV values (8.4°, 7.8°) that are slightly lower than those (8.7°, 9.4°) in the three averaged [(η^6-arene)Ru(η^6-$C_{20}H_{10}$)]$^{2+}$ complexes.

There are several changes in the corannulene C−C bond distances (Figures 2−5) in **3a**, **4**, **5**, and **6** as compared with those in **1** that illustrate the effect of (η^6-arene)Ru^{2+} or (η^6-arene)Os^{2+} coordination on the bowl shape. The most pronounced difference is observed (and calculated) for the rim C1−C2 bond of the metal-coordinated benzene ring. These distances for **3a**, **4**, **5**, and **6** are 1.43(1) 1.43(1) 1.43(1), and 1.42(2) Å and are calculated as 1.437, 1.436, 1.436, and 1.446 Å, respectively, which is longer than in the parent corannulene (1.402(5) Å).[5a] This lengthening of C1−C2 caused by (η^6-arene)Ru^{2+} or (η^6-arene)Os^{2+} coordination relieves strain in the curved bowl, thus allowing it to become slightly less curved. A similar lengthening of the C1−C2 distance (1.44(1) Å) was observed in [Cp*Ru(η^6-$C_{20}H_{10}$)][SbF_6][8] and [(COE)$_2$M(η^6-$C_{20}H_{10}$)]$^+$ (M = Rh, Ir).[11a] Such C−C bond length increases have been reported for many other η^6-arene metal complexes and are explained by charge transfer between the arene and metal complex that results in a net reduction in the C−C bond order.[37]

In contrast to the lengthening of the Ru-coordinated rim C−C bond distances, the noncoordinated rim C−C bonds in **3a**, **4**, **5**, and **6** are shorter (1.34(1), 1.36(1), 1.37(1), 1.37(1) Å for **3a**; 1.36(1), 1.37(1), 1.38(1), 1.37(1) Å for **4**; 1.37(1), 1.37(1), 1.37(1), 1.37(1) Å for **5**; 1.42(2), 1.32(2), 1.37(2), 1.35(2) Å for **6**) than that in free corannulene (1.402(5) Å). This shortening is also predicted by the calculations (1.383−1.393 Å). The same trend was also observed in the previously reported structure of

(33) Brockway, L. O.; Robertson, J. M. *J. Chem. Soc.* **1939**, 1324.

(34) Watkins, S. F.; Fronczek, F. R. *Acta Crystallogr., Sect. B* **1982**, *B38*, 270.

(35) Cabeza, J. A.; Adams, H.; Smith, A. J. *Inorg. Chim. Acta* **1986**, *114*, L17.

(36) Bennett, M. A.; McMahon, I. J.; Pelling, S.; Robertson, G. B.; Wichranasinghe, W. A. *Organometallics* **1985**, *4*, 754.

(37) Hubig, S. M.; Lindeman, S. V.; Kochi, J. K. *Coord. Chem. Rev.* **2000**, *200−202*, 831.

Table 3. ^{1}H NMR Chemical Shifts for Hydrogens on Corannulene[a] and Its Complexes[b]

complex	δ_{H1}	δ_{H2}	δ_{H3}	δ_{H4}	δ_{H5}
$[(\eta^6\text{-}C_6Me_6)Ru(\eta^6\text{-}C_{20}H_{10})][SbF_6]_2$ (**3a**)[c]	7.48 (6.4)	7.80 (7.5)	8.73 (8.8)	8.21 (8.5)	8.43 (8.8)
$[(\eta^6\text{-cymene})Os(\eta^6\text{-}C_{20}H_{10})][SbF_6]_2$ (**6**)[d]	7.91 (6.3)	7.80 (7.6)	8.72 (8.9)	8.10 (8.5)	8.39 (8.8)
$[Cp^*Ir(\eta^6\text{-}C_{20}H_{10})][BF_4]_2$[c,e]	7.98	7.97	8.74	8.18	8.46
$[Cp^*Ru(\eta^6\text{-}C_{20}H_{10})][O_3SCF_3]$[d,f]	6.59 (6.1)	7.60 (7.5)	8.18 (8.2)	7.95 (8.1)	8.11 (8.3)

[a] For $C_{20}H_{10}$ in CD_3NO_2, $\delta = 7.93$ ppm. [b] Chemical shifts are given in ppm; corannulene proton labels are given in Figure 1. GIAO-calculated δ values are given in parentheses. [c] In CD_3NO_2. [d] In CD_2Cl_2. [e] Ref 10. [f] Ref 7.

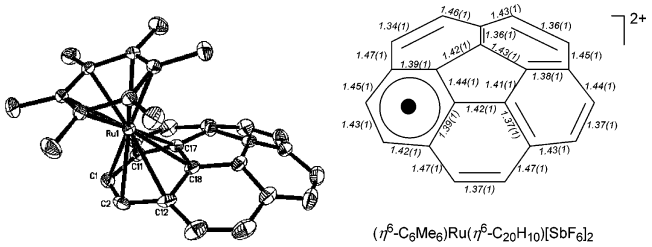

Figure 2. Thermal ellipsoid drawing of the $\mathbf{3}^{2+}$ cation in $[(\eta^6\text{-}C_6Me_6)Ru(\eta^6\text{-}C_{20}H_{10})][SbF_6]_2$ (**3a**). Ellipsoids are shown at the 30% probability level; hydrogen atoms are omitted for clarity. Bond distances in the $C_{20}H_{10}$ ligand are shown in the figure on the right (Å).

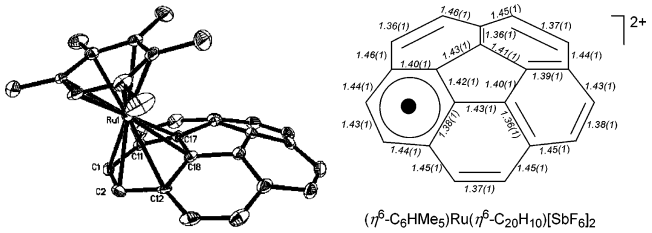

Figure 3. Thermal ellipsoid drawing of the $\mathbf{4}^{2+}$ cation in $[(\eta^6\text{-}C_6HMe_5)Ru(\eta^6\text{-}C_{20}H_{10})][SbF_6]_2$ (**4**). Ellipsoids are shown at the 30% probability level; hydrogen atoms are omitted for clarity. Bond distances in the $C_{20}H_{10}$ ligand are shown in the figure on the right (Å).

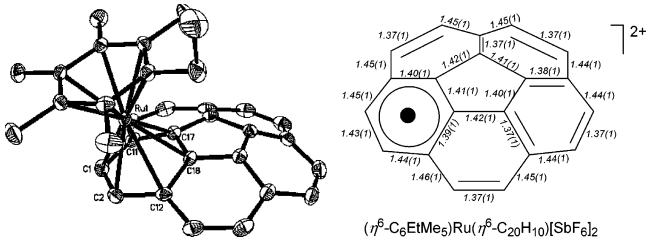

Figure 4. Thermal ellipsoid drawing of the $\mathbf{5}^{2+}$ cation in $[(\eta^6\text{-}C_6EtMe_5)Ru(\eta^6\text{-}C_{20}H_{10})][SbF_6]_2$ (**5**). Ellipsoids are shown at the 30% probability level; hydrogen atoms are omitted for clarity. Bond distances in the $C_{20}H_{10}$ ligand are shown in the figure on the right (Å).

$[Cp^*Ru(\eta^6\text{-}C_{20}H_{10})][SbF_6]$,[8] where the uncoordinated rim C−C bond lengths are 1.35(2), 1.34(2), 1.36(2), and 1.38(2) Å. The decrease in C−C bond lengths can be rationalized by assuming that six π-electrons are localized in the six-membered ring coordinated to (η^6-arene)Ru^{2+} or (η^6-arene)Os^{2+}. The remaining π-electrons in the corannulene ligand may then be localized in alternate single and double C−C bonds as shown in Figures 2−6. Such localization of electron density in noncoordinated portions of polyaromatic hydrocarbons that are η^6-coordinated to a transition metal fragment has been observed in several other complexes.[37]

The data in Table 4 show that there are two types of Ru−C(corannulene) distances in **3a**, **4**, and **5**: four short distances (∼2.23 Å) and two long distances (∼2.38 Å). This distinction is also apparent in the computational results. The four short

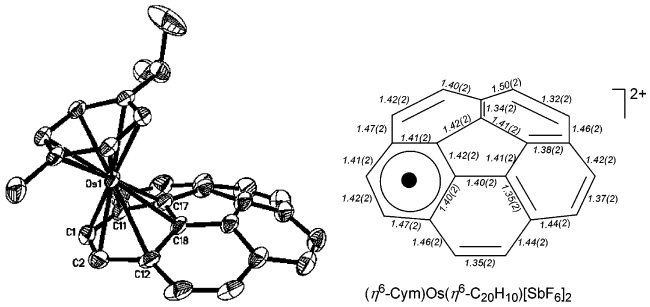

Figure 5. Thermal ellipsoid drawing of the $\mathbf{6}^{2+}$ cation in $[(\eta^6\text{-cymene})Os(\eta^6\text{-}C_{20}H_{10})][SbF_6]_2{\cdot}CH_2Cl_2$ (**6**·CH_2Cl_2). Ellipsoids are shown at the 30% probability level; hydrogen atoms are omitted for clarity. Bond distances in the $C_{20}H_{10}$ ligand are shown in the figure on the right (Å).

Ru−C distances to C1, C2, C17, and C18 are very similar to those of typical (η^6-arene)Ru^{2+} complexes, as in $(\eta^6\text{-}C_6Me_6)_2\text{-}Ru^{2+}$ (2.257 Å average). The two long Ru−C distances to C11 and C12 are significantly longer by ∼0.1 Å than the normal Ru−C distance in (η^6-arene)Ru^{2+} complexes. Those two types of Ru−C bond distances reflect folding of the coordinated ring along the C11−C12 vector. This same pattern of Ru−C distances was observed in $[Cp^*Ru(\eta^6\text{-}C_{20}H_{10})][SbF_6]$,[8] where the four short Ru−C distances are 2.221(7), 2.211(7), 2.231(8), and 2.222(8) Å, while the two long Ru−C bonds are 2.382(7) and 2.361(6) Å. Similarly, there are four short and two long Os−C(corannulene) bond distances in **6**. Comparison of the calculated Ru−C bond lengths with the crystallographic data (Table 4) reveals a systematic overestimation of the distances by the theoretical model by ca. 0.02 to 0.08 Å (0.04 Å on average). The overestimation was previously observed by us for $[Cp^*Ru(\eta^6\text{-}C_{20}H_{10})][SbF_6]$;[8] in fact, Ru−C distances in this case were calculated to be too long by ca. 0.1 Å with the Becke3LYP/GEN model. There is no doubt that at least a part of the discrepancy between the experimental and calculated lengths comes from the simplicity of the isolated dication model as compared to the real system, which includes counter anions and solvent molecules embedded in the crystals. We were, however, pleased to find that moving from the Becke3/LYP to the PBE functional reduced the overestimation of these bond lengths by ca. 50%.

A parameter that is used to describe the overall curvature of a buckybowl is the bowl depth, which is the distance between the centroid of the five core carbon atoms and the plane defined by the 10 tertiary rim carbon atoms. It is 0.83 Å in **3a** and **4**, 0.84 Å in **5**, and 0.78 Å in **6** (Table 5), just slightly less than that in free corannulene (**1**, 0.87 Å); the bowl in **3a**, **4**, and **5** is apparently deeper than that (0.78 Å) in $[Cp^*Ru(\eta^6\text{-}C_{20}H_{10})]\text{-}[SbF_6]$.[8] The even greater flattening of the corannulene in $[(Cp^*Ru)_2(\mu_2\text{-}\eta^6\text{:}\eta^6\text{-}C_{20}H_{10})][PF_6]_2$ is evident in its bowl depth of only 0.42 Å.[9] In the flat $[(Cp^*Ru)_2(\mu_2\text{-}\eta^6\text{:}\eta^6\text{-}C_{20}H_{10})][SbF_6]_2$ salt, the bowl depth is essentially zero.[8]

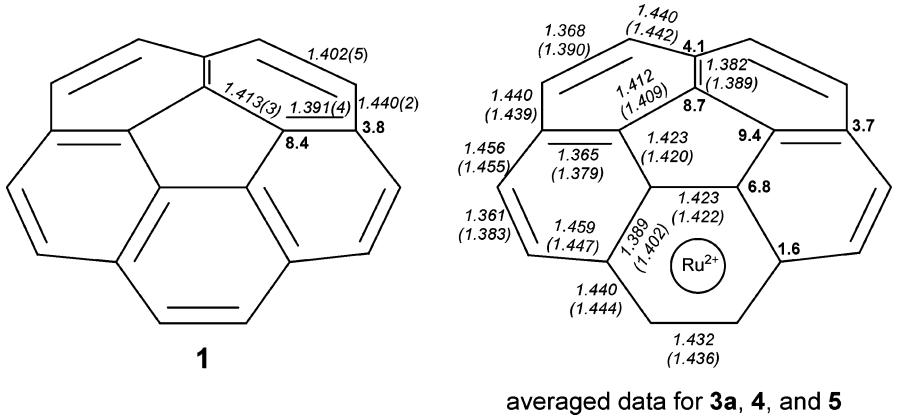

Figure 6. POAV pyramidalization angles (in boldface; deg) and C−C bond lengths (Å) in corannulene (**1**)[5] and averaged data for **3a**, **4**, and **5** (calculated lengths in parentheses).

Table 4. Comparison of M−C(Corannulene) Bond Distances in Complexes 3−6[a]

complex	M1−C1 (Å)	M1−C2 (Å)	M1−C11 (Å)	M1−C12 (Å)	M1−C17 (Å)	M1−C18 (Å)
3a (M = Ru)	2.230(9)	2.218(9)	2.367(9)	2.393(9)	2.225(8)	2.247(9)
	2.248	*2.244*	*2.445*	*2.450*	*2.269*	*2.273*
4 (M = Ru)	2.225(7)	2.232(7)	2.373(7)	2.414(7)	2.222(7)	2.236(7)
	2.245	*2.250*	*2.448*	*2.448*	*2.274*	*2.278*
5 (M = Ru)	2.229(5)	2.230(5)	2.398(5)	2.380(5)	2.245(5)	2.242(4)
	2.251	*2.247*	*2.454*	*2.448*	*2.278*	*2.273*
6·CH_2Cl_2 (M = Os)	2.236(13)	2.218(13)	2.404(14)	2.396(10)	2.251(11)	2.258(10)
	2.236	*2.224*	*2.462*	*2.456*	*2.260*	*2.262*
[Cp*Ru(η^6-$C_{20}H_{10}$)][SbF_6][8]	2.221(7)	2.211(7)	2.382(7)	2.361(8)	2.231(8)	2.222(8)
	2.239	*2.239*	*2.241*	*2.241*	*2.277*	*2.277*

[a] PBE/GEN-calculated distances in italics.

Table 5. Comparison of Crystal Structure Parameters in Complexes 3−6

	1[5]	**3a**	**4**	**5**	**6**·CH_2Cl_2	[Cp*Ru(η^6-$C_{20}H_{10}$)][SbF_6][8]
bowl depth	0.87 Å	0.83 Å	0.83 Å	0.84 Å	0.78 Å	0.78 Å
fold angle (coordinated 6-ring)		11.8°	12.8°	12.4°	12.5°	12.0°
fold angle (noncoordinated 6-rings)	8.8−11.2°	9.7−13.9 °	10.4−12.8°	9.2−13.5°	8.3−12.4°	8.8−12.6°

Another interesting feature of the carbon framework in **3a**, **4**, **5**, and **6** is the folding of the corannulene six-membered ring to which the (η^6-arene)Ru^{2+} or (η^6-arene)Os^{2+} unit is coordinated (Table 5). The fold occurs along the C11−C12 vector in a way that moves C1 and C2 up toward the Ru, resulting in an angle (11.8° for **3a**, 12.8° for **4**, 12.4° for **5**, and 12.5° for **6**) between the planes defined by C1, C2, C12, C11 and C12, C18, C17, C11. All of the noncoordinated six-membered rings are folded similarly with fold angles in the range 9.7−13.9° for **3a**, 10.4−12.8° for **4**, 9.2−13.5° for **5**, and 8.3−12.4° for **6**. It should be noted that the six-membered rings in free corannulene are folded in a similar manner with fold angles of 8.8−11.2°.[5] In [Cp*Ru(η^6-$C_{20}H_{10}$)][SbF_6],[8] the fold angle (12.0°) of the coordinated six-membered ring and the fold angles (8.8−12.6°) of the noncoordinated six-membered rings are very similar to those in complexes **3a**, **4**, **5**, and **6**.

Reactions of [(η^6-C_6Me_6)Ru(η^6-$C_{20}H_{10}$)][SbF_6]$_2$ (3a) with Nucleophiles/Bases. Deprotonation of [Ru(η^6-C_6Me_6)$_2$]$^{2+}$ with ^{t}BuOK is known to give the *o*-xylylene complex of ruthenium(0), Ru(η^6-C_6Me_6)[η^4-$C_6Me_4(CH_2)_2$].[38] The same reaction of **3a** with 2 equiv of ^{t}BuOK in THF conducted at −78 °C resulted in a rapid change in color from yellow to red; within 5 min, the color then changed to brown, and the ^{1}H NMR spectrum of the product showed that all of the corannulene was present as the free compound. Similar reactions of **3a** with CH_3ONa in methanol[39] and with NEt_3 in CD_3NO_2[40] also resulted in decomposition of the complex and release of free corannulene. In another type of reaction, it is known that the complexes [Ru(η^6-C_6H_6)$_2$]$^{2+}$ (M = Fe, Ru, Os) react rapidly and reversibly with tertiary phosphines to form cyclohexadienyl phosphonium ring adducts.[41] The same type of reaction of **3a** with a 5-fold excess of a phosphine (PMe_3, PEt_3, P(*n*-Bu)$_3$, $PPhMe_2$, or PPh_2Me) resulted in a rapid change of color from yellow to red; then, within 1−2 h, the color turned back to yellow. ^{1}H NMR spectra of the products showed that a mixture of products had formed, but only a small amount of uncoordinated corannulene was detected. For the specific case of the PEt_3 reaction, the first-formed red compound exhibited ^{1}H NMR resonances (6.7−7.7 ppm) for hydrogens on corannulene that are shifted upfield relative to those of starting complex **3a** (7.5−8.7 ppm). Also, the singlet and four doublets of the corannulene in **3a** changed to at least eight groups of peaks, perhaps indicating the formation of isomers resulting from PEt_3 addition to different carbon atoms in the corannulene ring. The ^{1}H NMR signal of the C_6Me_6 group in the red compound remained as a singlet at nearly the same chemical shift as that in **3a**; this indicates that the PEt_3 did not add to the C_6Me_6 ligand. The ^{1}H NMR spectrum of the final yellow compound exhibited corannulene resonances near those

(38) Lai, Y.-H.; Tam, W.; Vollhardt, K. P. C. *J. Organomet. Chem.* **1981**, *216*, 97.

(39) Grundy, S. L.; Smith, A. J.; Adams, H.; Maitlis, P. M. *J. Chem. Soc., Dalton Trans.* **1984**, 1747.

(40) Bennett, M. A., Goh, L. Y.; Willis, A. C. *J. Am. Chem. Soc.* **1996**, *118*, 4984.

(41) Domaille, P. J.; Ittel, S. D.; Jesson, J. P.; Sweigart, D. A. *J. Organomet. Chem.* **1980**, *202*, 191.

of the starting complex **3a**, but the pattern of peaks was much more complicated with at least eight groups of peaks. In the C_6Me_6 region, several peaks were observed indicating that the PEt_3 had also added to the C_6Me_6. In the ^{31}P NMR spectrum of the yellow compound, there were at least 14 resonances, some of which may be coupled to each other, in the range 10 to 42 ppm. We were unable to separate or crystallize any of the products of the reactions of **3a** with phosphines. This is unfortunate because one would expect the PR_3 addition to occur on the side of the bowl opposite that of the $(\eta^6\text{-}C_6Me_6)Ru^{2+}$; this should cause the corannulene bowl to invert, resulting in a cyclohexadienyl unit in the corannulene that is coordinated to the $(\eta^6\text{-}C_6Me_6)Ru^{2+}$ group on the *endo* side of the bowl with the PR_3 group on the *exo* side. Confirmation of such structural changes depends on the isolation of products from future studies of reactions of η^6-corannulene complexes with nucleophiles.

Conclusions

The η^6-corannulene complexes $[(\eta^6\text{-}C_6Me_6)Ru(\eta^6\text{-}C_{20}H_{10})]X_2$ (**3a**, X = SbF_6; **3b**, X = PF_6; **3c**, X = BF_4), $[(\eta^6\text{-}C_6HMe_5)Ru(\eta^6\text{-}C_{20}H_{10})](SbF_6)_2$ (**4**), $[(\eta^6\text{-}C_6EtMe_5)Ru(\eta^6\text{-}C_{20}H_{10})](SbF_6)_2$ (**5**), and $[(\eta^6\text{-cymene})Os(\eta^6\text{-}C_{20}H_{10})](SbF_6)_2$ (**6**) that are described in this paper are more stable to air exposure than any previously reported η^6-corannulene complexes. This stability together with previous characterizations of η^6-corannulene complexes of Cp^*Ru^+, Cp^*Ir^{2+}, and $[(COE)_2M]^+$ (M = Rh or Ir) indicate that cationic metal units bind more strongly to corannulene than neutral fragments such as $Cr(CO)_3$ and $W(CO)_3$, which show no evidence for coordination to corannulene.[10,42] It is somewhat surprising that the slightly flattened structure of the corannulene in the +2 complexes $(\eta^6\text{-arene})M(\eta^6\text{-}C_{20}H_{10})^{2+}$ (M = Ru, Os) is so similar to that in the +1 complex $Cp^*Ru(\eta^6\text{-}C_{20}H_{10})^+$, because the $(\eta^6\text{-}C_6Me_6)Ru^{2+}$ unit is much less electron-rich than Cp^*Ru^+; this is indicated by the substantially higher ν(CO) values for $(\eta^6\text{-}C_6Me_6)Ru(CO)_2Cl^+$ (2100, 2063 cm^{-1} in KBr)[43] than for $Cp^*Ru(CO)_2Cl$ (2025, 1975 cm^{-1} in CH_2Cl_2).[44] The corannulene structures in all of the complexes are reproduced well by the computational studies at both B3LYP/GEN and PBE/GEN levels of theory, with the latter reproducing the metal−carbon distances much better than the former. Although it was not possible to isolate and fully characterize products of the reactions of $(\eta^6\text{-}C_6Me_6)Ru(\eta^6\text{-}C_{20}H_{10})^{2+}$ with phosphines (PR_3), it is evident that the $(\eta^6\text{-}C_6Me_6)Ru^{2+}$ unit does activate the corannulene to react with these nucleophiles.

Acknowledgment. This work was supported by the U.S. Department of Energy under Contract No. DE-AC02-07CH11358 with Iowa State University and through Grant DE-FG02-04ER15514 to Mississippi State University.

Supporting Information Available: NMR spectra of **3a**, UV−vis spectrum of **3c**, crystallographic data (CIF) for **3a**, **4**, **5**, and **6**·CH_2Cl_2, and computational results for $\mathbf{3}^{2+}$, $\mathbf{4}^{2+}$, $\mathbf{5}^{2+}$, $\mathbf{6}^{2+}$, and $Cp^*Ru(\eta^6\text{-}C_{20}H_{10})^+$. This material is available free of charge via the Internet at http://pubs.acs.org.

OM0610795

(42) Stoddart, M. W.; Brownie, J. H.; Baird, M. C.; Schmider, H. L. *J. Organomet. Chem.* **2005**, *690*, 3440.
(43) Roder, K.; Werner, H. *Chem. Ber.* **1989**, *122*, 833.
(44) Nagashima, H.; Mukai, K.; Shiota, Y.; Yamaguchi, K.; Ara, K.; Fukahori, T.; Suzuki, H.; Akita, M.; Morooka, Y.; Itoh, K. *Organometallics* **1990**, *9*, 799.